

## ANALYSIS OF THE DEFORMATIONS OF THE SLIDING LAYERS OF THE THREAD CONDUCTOR WITH DIFFERENT ELEMENTS OF RING SPINNING MACHINES

<https://doi.org/10.5281/zenodo.8059594>

DSc. Professor **K. Jumaniyazov**

*Uzpakhtsanoat Scientific Center, Tashkent, Uzbekistan*

Ph.D. associate professor **G'.Kh.Djumabaev**

*Chirchik State Pedagogical University, Chirchik, Uzbekistan*

*[djumabaev.g@cspi.uz](mailto:djumabaev.g@cspi.uz)*

### Annotation

*Mathematical expressions representing thread deformations of three-layer belt elements (bushes) of yarn transfer with different components on a ring spinning machine were obtained, connection graphs were constructed. Based on the analysis of the obtained graphs, it was determined that the total displacement of the belt bushings of the thread conductor, that is, the deformation along the radius does not exceed  $(0.35 \div 0.95) \cdot 10^{-3}m$ . At the same time, it is recommended that the size of the outer belt bushing is  $(1.15 \div 1.32)$  times smaller than the size of the second layer of bushings, and the size of the third (outer) belt bushing should be  $(1.35 \div 1.45)$  times smaller than the size of the bushing.*

When the thread of different layers passes through the conductor, its tension changes and affects the belt elements of the conductor. In this case, it is ensured that the thread protection effect is smooth due to the overall deformation of the interlocking thread conductor layers. In that occasion, the change in thread tension is sufficiently decreased.

We study the initial priority of the three-layer thread conductor shown in Fig. 1 [2, 3, 4]. Let's assume that the thread conductor has three layers. Its cross-section is shown in Figure 2

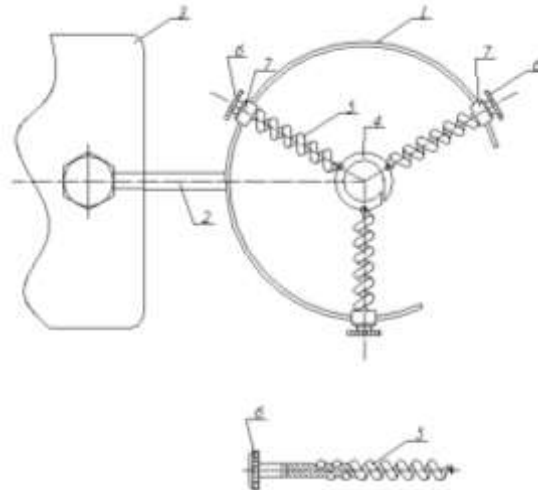


**Figure 1. Threader with yielding element**

To learn

$$E_2 \delta_2 \ll E_1 \delta_1; \delta_1 \ll \delta_2,$$

get that the conditions are true. Here  $E_1$  - the modulus of elasticity of the outer layers;  $E_2$  - modulus of elasticity of the inner layer;  $\delta_1, \delta_2$  - shows the thicknesses of the layers, respectively

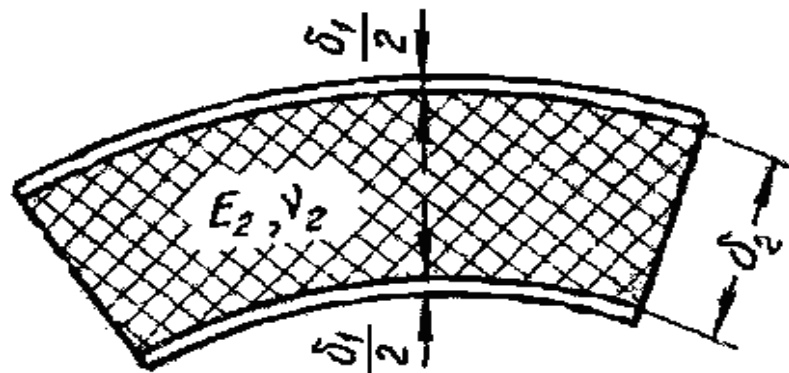


**Figure 2. The cross-sectional surface of the thread conductor**

Considering the string conductor as a shell, we believe that the Kirchhoff-Liav hypothesis is valid for it. We enter  $\alpha_1, \alpha_2, z$  coordinate system for each layer. In this case, we accept the calculation scheme in the form of Figure 3.

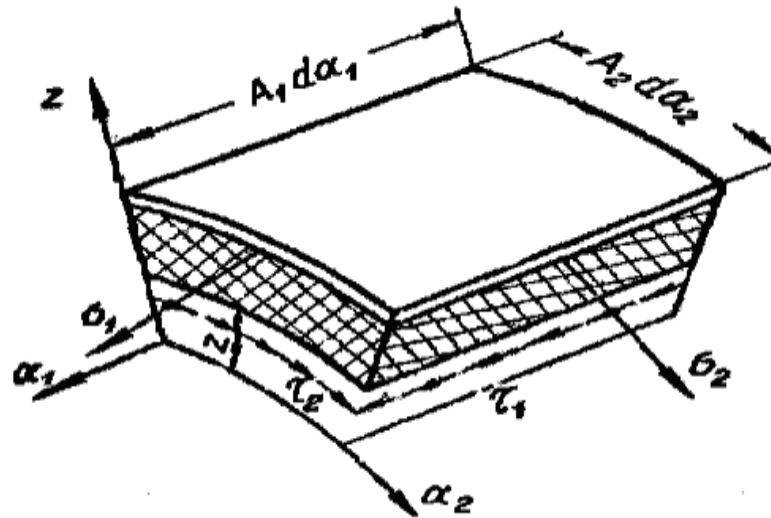


**Figure 3. Calculation scheme of a three-layer thread conductor**

Based on the Kirchhoff-Liav hypothesis, the stress-strain state of the three-layer shell is determined by  $\sigma_i = \sigma_i(\varepsilon_i)$  the formula. Therefore, at each point in the sample elongation diagram  $\sigma_i$  and  $\varepsilon_i$  are constructed. In general, voltage and deformation are connected through the formula

$$\sigma_{ii} = (K - 2E_c/9)\varepsilon_0 + 2E_c\varepsilon_{ii}/3 \quad (i=1,2,3), \quad (1)$$

$K$  in this formula is related to the deformation deviator as follows

$$K = \frac{E}{3(1-2\nu)}; \quad \varepsilon_0 = \varepsilon_{11} + \varepsilon_{22} + \varepsilon_{33}. \quad (2)$$

In general, formula (1) expresses the nonlinearity between voltage and deformation. It  $E_c - 3G = 3E/(2(1+\nu))$  overlaps with the expressions of the theory of elasticity. After the voltage and deformation are determined, the forces and moments will be determined. We present the geometric connections for three-layer shells in the form below:

$$\begin{aligned} \varepsilon_1 &= \frac{1}{A_1} \frac{\partial u}{\partial \alpha_1} + \frac{\nu}{A_1 A_2} \frac{\partial A_1}{\partial \alpha_2} + \frac{w}{R_1}; \\ \varepsilon_2 &= \frac{1}{A_2} \frac{\partial v}{\partial \alpha_2} + \frac{u}{A_1 A_2} \frac{\partial A_2}{\partial \alpha_1} + \frac{w}{R_2}; \\ 2\varepsilon_3 &= \frac{A_2}{A_1} \frac{\partial}{\partial \alpha_1} \left( \frac{v}{A_2} \right) + \frac{A_1}{A_2} \frac{\partial}{\partial \alpha_2} \left( \frac{u}{A_1} \right). \end{aligned} \quad (3)$$

where  $A_1(\alpha_1), A_2(\alpha_1)$  – Lamé coefficients;  $R_1(\alpha_1), R_2(\alpha_1)$  – are the main radius of curvature, and for a cylindrical shell they are equal to each other.  $A_i$  and  $k_i = 1/R_i (i=1,2)$  quantities are determined from the Gauss-Kodatsi equations

$$\begin{aligned} \frac{1}{A_1} \frac{\partial k_2}{\partial \alpha_1} &= (k_1 - k_2) \frac{1}{A_1 A_2} \frac{\partial A_2}{\partial \alpha_1}; \\ \frac{1}{A_1} \frac{\partial}{\partial \alpha_1} \left( \frac{1}{A_1} \frac{\partial A_2}{\partial \alpha_1} \right) &= -k_1 k_2 A_2. \end{aligned} \quad (4)$$

Components of bending deformations with displacements and torsions

$$\begin{aligned} \chi_1 &= -\frac{1}{A_1} \frac{\partial}{\partial \alpha_1} \left( \frac{1}{A_1} \frac{\partial \Phi}{\partial \alpha_1} \right) - \frac{1}{A_1 A_2^2} \frac{\partial A_1}{\partial \alpha_2} \frac{\partial \Phi}{\partial \alpha_2}; \\ \chi_2 &= -\frac{1}{A_2} \frac{\partial}{\partial \alpha_2} \left( \frac{1}{A_2} \frac{\partial \Phi}{\partial \alpha_2} \right) - \frac{1}{A_2 A_1^2} \frac{\partial A_2}{\partial \alpha_1} \frac{\partial \Phi}{\partial \alpha_1}; \\ \chi_3 &= -\frac{1}{A_1 A_2} \left[ \frac{\partial^2 \Phi}{\partial \alpha_1 \partial \alpha_2} - \frac{1}{A_2} \frac{\partial A_2}{\partial \alpha_1} \frac{\partial \Phi}{\partial \alpha_2} \right] - \frac{1}{A_1} \frac{\partial A_1}{\partial \alpha_2} \frac{\partial \Phi}{\partial \alpha_1}; \\ \gamma_1 &= -\frac{1}{A_1} \frac{\partial}{\partial \alpha_1} (\Phi - w); \quad \gamma_2 = -\frac{1}{A_2} \frac{\partial}{\partial \alpha_2} (\Phi - w), \end{aligned} \quad (5)$$

are linked by the formulas, and the following angular functions are introduced to determine the angular deformations:

$$\varphi = -\frac{1}{A_1} \frac{\partial \Phi}{\partial \alpha_1}; \quad \phi = -\frac{1}{A_2} \frac{\partial \Phi}{\partial \alpha_2}. \quad (6)$$

When obtaining the general equations for determining the voltage-deformation state of three-layer shells, separate equations are derived for each layer. Boundary conditions are then imposed on each contour. In this case, the order of the equations is determined by the number of layers.

We use Lagrange's variational principle to form the equation. As a result of a series of mathematical transformations, we create the following system of equations

$$\begin{aligned} \frac{\partial T_{11}}{\partial \alpha_1} + \psi(T_{11} - T_{22}) + \frac{\partial S}{\partial \alpha_2} + k_1(Q_{11} + \frac{\partial H}{\partial \alpha_2}) + q_1 &= 0; \\ \frac{\partial S}{\partial \alpha_1} + 2\psi(S + k_1 H) + \frac{\partial T_{22}}{\partial \alpha_2} + k_2(Q_{22} + \frac{\partial H}{\partial \alpha_1}) + q_2 &= 0; \\ \frac{\partial Q_{11}}{\partial \alpha_1} + \psi Q_{11} + \frac{\partial Q_{22}}{\partial \alpha_2} - k_1 T_{11} - k_2 T_{22} + q_3 &= 0; \\ \frac{\partial M_{11}}{\partial \alpha_1} + \psi(M_{11} - M_{22}) + \frac{\partial H}{\partial \alpha_2} - Q_{11} &= 0; \\ \frac{\partial H}{\partial \alpha_1} + 2\psi H + \frac{\partial M_{22}}{\partial \alpha_2} + Q_{22} &= 0. \end{aligned} \quad (7)$$

Components of force vector

$$N = [T_{11}, T_{22}, M_{11}, M_{22}, S, H]^T \quad (8)$$

through generalized deformations associated with an expression:

$$N = [C]\varepsilon, \quad (9)$$

Here are  $[C]$ ,  $c_{ij}$  the elements of the matrix.

$$c_{11}^{(k)} = \int_{-h/2}^{h/2} \frac{E_1 z^k}{1-\nu_1 \nu_2} dz; \quad c_{22}^{(k)} = \int_{-h/2}^{h/2} \frac{E_2 z^k}{1-\nu_1 \nu_2} dz; \quad c_{12}^{(k)} = \int_{-h/2}^{h/2} \frac{\nu_2 E_1 z^k}{1-\nu_1 \nu_2} dz; \quad c_{33}^{(k)} = \int_{H\Xi}^{h/2} z^2 dz. \quad (10)$$

are determined from formulas.

We assume that the displacements in the layers are respectively related as follows:

1. For the upper layer

$$w_B = w_1, \quad u_B = u_1 - (z + h + t/2) \frac{\partial w_1}{\partial x}, \quad v_B = v_1 - (z + h + t/2) \frac{\partial w_1}{\partial y}, \quad (11)$$

$u_1, v_1, w_1$  – represents displacements in the upper layer.

2. For the bottom layer

$$w_H = w_2, \quad u_H = u_2 - (z - h - t/2) \frac{\partial w_2}{\partial x}, \quad v_H = v_2 - (z - h - t/2) \frac{\partial w_2}{\partial y}, \quad (12)$$

$u_2, v_2, w_2$  – displacements in the lower layer.

3. For the middle layer

$$w_c = w, \quad u_c = \frac{1}{2}(u_1 + u_2) - \frac{z}{2h}(u_1 - u_2 - t \frac{\partial w}{\partial x}), \quad v_c = \frac{1}{2}(v_1 + v_2) - \frac{z}{2h}(v_1 - v_2 - t \frac{\partial w}{\partial y}). \quad (13)$$

Boundary conditions for  $\alpha_1 = const$  while the boundary is free

$$T_{11} = S = Q_{11} + \frac{1}{A_2} \frac{\partial H}{\partial \alpha_2} = 0;$$

tightly clamped

$$u = v = w = \varphi = 0;$$

in the transverse direction, it is pulled to the hinge, and in the tangential direction, it is tightly clamped

$$u = v = w = 0;$$

tightly clamped in the transverse direction and free in the tangential direction

$$T_{11} = S = w = \varphi = 0$$

and etc.

Precedence equations with respect to displacements for three-layer shells

$$\begin{aligned}
 & \frac{\partial^2 u_\alpha}{\partial x^2} + \frac{1-\mu}{2} \frac{\partial^2 u_\alpha}{\partial y^2} + \frac{1+\mu}{2} \frac{\partial^2 v_\alpha}{\partial x \partial y} - \frac{\partial}{\partial x} \left( \frac{w}{R_1} + \mu \frac{w}{R_2} \right) = 0, \\
 & \frac{\partial^2 v_\alpha}{\partial y^2} + \frac{1-\mu}{2} \frac{\partial^2 v_\alpha}{\partial x^2} + \frac{1+\mu}{2} \frac{\partial^2 u_\alpha}{\partial x \partial y} - \frac{\partial}{\partial y} \left( \frac{w}{R_2} + \mu \frac{w}{R_1} \right) = 0, \\
 & \frac{Bh}{G_3} \left( \frac{\partial^2 u_\beta}{\partial x^2} + \frac{1-\mu}{2} \frac{\partial^2 u_\beta}{\partial y^2} + \frac{1+\mu}{2} \frac{\partial^2 v_\beta}{\partial x \partial y} \right) - u_\beta + (h+0.5t) \frac{\partial w}{\partial x} = 0, \\
 & \frac{Bh}{G_3} \left( \frac{\partial^2 v_\beta}{\partial y^2} + \frac{1-\mu}{2} \frac{\partial^2 v_\beta}{\partial x^2} + \frac{1+\mu}{2} \frac{\partial^2 u_\beta}{\partial x \partial y} \right) - v_\beta - (h+0.5t) \frac{\partial w}{\partial y} = 0, \\
 & -2B(h+0.5t) \nabla^2 \left( \frac{\partial u_\beta}{\partial x} + \frac{\partial v_\beta}{\partial y} \right) - 2D \nabla^4 w + \frac{2B}{R_1} \left( \frac{\partial u_\alpha}{\partial x} + \mu \frac{\partial v_\alpha}{\partial y} - \frac{w}{R_1} - \mu \frac{w}{R_2} \right) + \\
 & + \frac{2B}{R_2} \left( \frac{\partial v_\alpha}{\partial y} + \mu \frac{\partial u_\alpha}{\partial x} - \frac{w}{R_2} - \mu \frac{w}{R_1} \right) + N_x^0 \frac{\partial^2 w}{\partial x^2} + N_y^0 \frac{\partial^2 w}{\partial y^2} + 2T^0 \frac{\partial^2 w}{\partial x \partial y} = 0.
 \end{aligned} \tag{14}$$

will be in the form. Let's consider a three-layer shell-like structural element with identical outer layers. We denote the radius of curvature by  $R_1$  and  $R_2$ , respectively. Here are the formulas that determine the displacements for the outer layers, losing priority:

for the upper layer [6, 7]

$$w_B = w_1, u_B = u_1 - (z+h+t/2) \frac{\partial w_1}{\partial x}, v_B = v_1 - (z+h+t/2) \frac{\partial w_1}{\partial y}, \tag{15}$$

for the bottom layer

$$w_H = w_2, u_H = u_2 - (z-h-t/2) \frac{\partial w_2}{\partial x}, v_H = v_2 - (z-h-t/2) \frac{\partial w_2}{\partial y}, \tag{16}$$

where  $u_1, v_1, w_1$  – are displacements in the upper layer,  $u_2, v_2, w_2$  – are displacements in the lower layer. And for the middle layer we get the formulas:

$$w_c = w, u_c = \frac{1}{2}(u_1 + u_2) - \frac{z}{2h}(u_1 - u_2 - t \frac{\partial w}{\partial x}), v_c = \frac{1}{2}(v_1 + v_2) - \frac{z}{2h}(v_1 - v_2 - t \frac{\partial w}{\partial y}). \tag{17}$$

The system of equations presented above

$$\begin{aligned}
 & 2B(h + \frac{t}{2})^2 \nabla^8 w + (1 - \frac{Bh}{G_3} \nabla^2) [2D \nabla^8 w + 2(1 - \mu^2) B (\frac{1}{R_1} \frac{\partial^2}{\partial y^2} + \\
 & + \frac{1}{R_2} \frac{\partial^2}{\partial x^2})^2 w - \nabla^4 (N_x^0 \frac{\partial^2 w}{\partial x^2} + N_y^0 \frac{\partial^2 w}{\partial y^2} + 2T^0 \frac{\partial^2 w}{\partial x \partial y})] = 0
 \end{aligned} \tag{18}$$

can be seen. The solution of this equation will look:

$$w = A \sin(m\pi x/a) \sin(n\pi y/b) \tag{19}$$

Substituting this expression into the above equation, after certain mathematical transformations we obtain the formula for the critical force.

$$N_k = \frac{\pi^2 D \left(\frac{m^2}{a^2} + \frac{n^2}{b^2}\right)^2}{\frac{m^2}{a^2} \left(1 + \pi^2 \left(\frac{m^2}{a^2} + \frac{n^2}{b^2}\right)^2\right) \frac{D}{K}} \quad (20)$$

In this formula D-bending stiffness of the three-layer shell; B-coefficient of uniformity in elongation and compression; K-coefficient of singularity in the transverse displacement of the three-layer shell;  $G_2$  - the modulus of elasticity in the displacement of the middle layer

$$D = \frac{E_1(\delta_1^3 - \delta_2^3)}{12(1 - \nu_1^2)}, \quad K = G_2 \delta_2, \quad B = \frac{E_1 \delta_1}{1 - \nu_1^2} \quad (21)$$

$n = 1$  critical force

$$N_k = \frac{\pi^2 D \left(\frac{m^2}{a^2} + \frac{1}{b^2}\right)^2}{\frac{m^2}{a^2} \left(1 + \pi^2 \left(\frac{m^2}{a^2} + \frac{1}{b^2}\right)^2\right) \frac{D}{K}} \quad (22)$$

is determined from the formula. We check this expression for a minimum against the  $\frac{m^2}{a^2}$  argument. The function reaches its minimum at the following value of the  $\frac{m^2}{a^2}$  argument

$$\frac{m^2}{a^2} = \frac{Kb^2 + \pi^2 D}{b^2 (Kb^2 - \pi^2 D)}$$

Then the minimum value of the critical force

$$(N_k)_{\min} = \frac{4\pi^2 b^2 D}{\left(b^2 + \frac{\pi^2 D}{K}\right)^2}$$

is determined from the formula. We introduce the following definition

$$\zeta = \frac{a^2 Kb^2 + \pi^2 D}{b^2 Kb^2 - \pi^2 D}$$

critical force at  $m = 1$

$$N_k = \frac{\pi^2 DK(a^2 + b^2)^2}{b^2 K^2 a^2 b^2 + \pi^2 (a^2 + b^2) D}$$

is found from the expression At an arbitrary value of  $m$ , the parameter  $\zeta$  is determined from the formula.

$$\zeta = \frac{Kb^2 + \pi^2 D}{Kb^2 - \pi^2 D} \sqrt{m^2 (m+1)^2 - \frac{\pi^2 D}{b^2 K} \left(m^2 + \frac{a^2}{b^2}\right) \left((m+1)^2 + \frac{a^2}{b^2}\right)^2}$$

The graphs representing the interrelationship of  $\zeta$  and  $m$  parameters are presented in Figure 4.

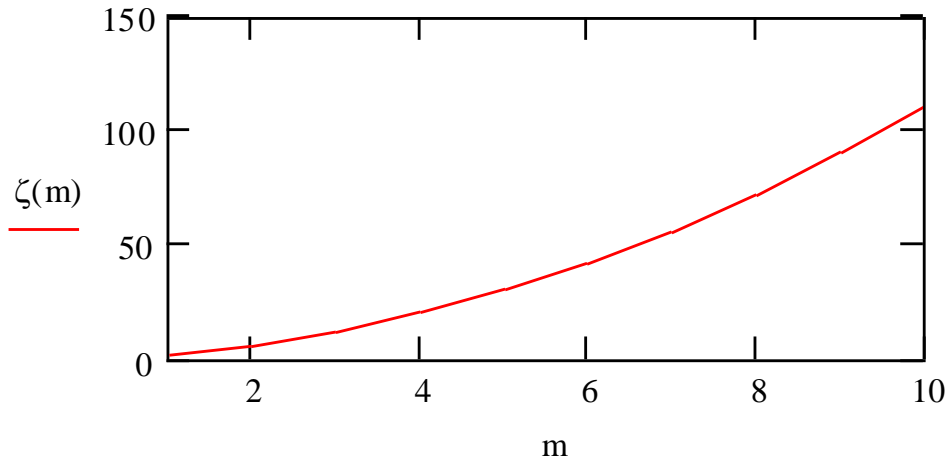


Figure 4. Graphs representing the dependence of the parameter  $\zeta$  on  $m$

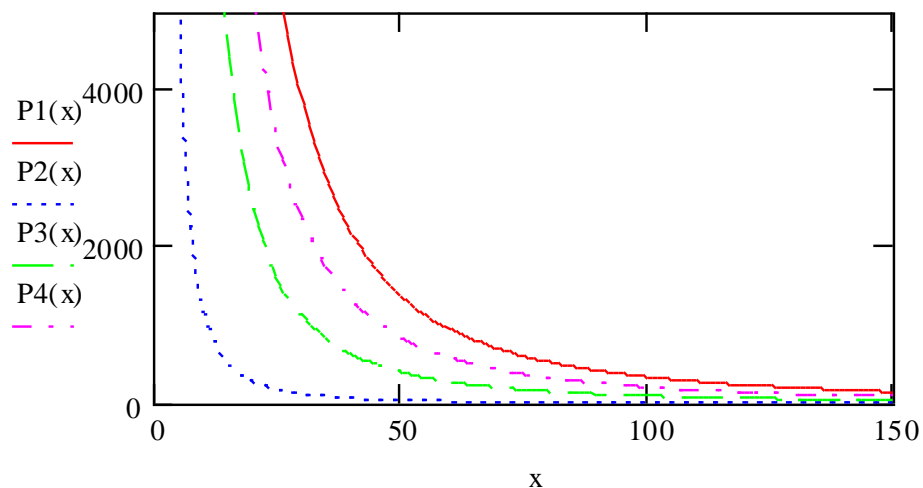


Figure 5. Dependence of critical forces on relative thickness ( $x = b/h$ ).

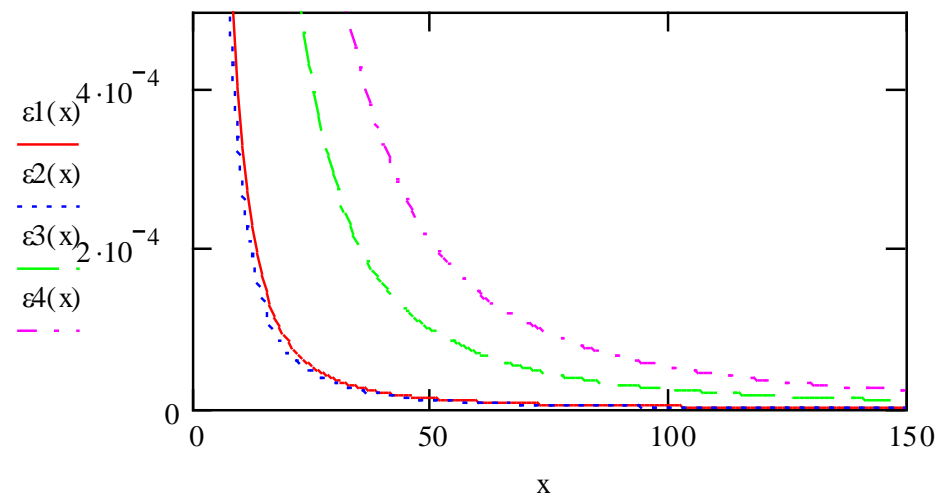


Figure 6. Dependence of deformation intensity on relative thickness ( $x = b/h$ ).



As another important issue, we investigate the priority of the three-layer cylindrical shell. In this case, the equations characterizing the priority

$$\begin{aligned} \kappa \frac{d^2 u_\beta}{d\xi^2} - u_\beta + (h + \frac{t}{2}) \frac{\pi}{a} \frac{dw}{d\xi} &= 0 \\ - \frac{a}{\pi(h + \frac{t}{2})} \frac{d^2 u_\beta}{d\xi^2} - r \frac{d^4 w}{d\xi^4} - \varphi \frac{d^2 w}{d\xi^2} &= 0 \end{aligned} \quad (23)$$

will be displayed. Here  $\varphi$  is a parameter characterizing the critical load, with

$$N = 2\varphi\pi^2 B(h + 0.5t)^2 / a^2, \quad B = Et / (1 - \mu^2)$$

linked by formula. We introduce the following definitions:

$$\xi = \pi x / a, \quad k = Bh\pi^2 / a^2 G_3, \quad r = t^2 / 12(h + 0.5t)^2.$$

We assume

$$w = \frac{du_\beta}{dx} = 0 \quad \xi = 0, \quad \xi = \pi.$$

boundary conditions for the hinged connection. The system of equations (23) is reduced to a system of differential equations of the first order. To do this

$$y_1 = u_\beta, \quad y_2 = \frac{du_\beta}{dx}, \quad y_3 = \frac{d^2 u_\beta}{dx^2}, \quad y_4 = w, \quad y_5 = \frac{dw}{dx}, \quad y_6 = \frac{d^2 w}{dx^2}, \quad y_7 = \frac{d^3 w}{dx^3}.$$

we create a system of simple, first-order differential equations defining the problem, including the notations:

$$\begin{aligned} \frac{dy_1}{d\xi} &= y_2; \\ \frac{dy_2}{d\xi} &= y_1 / k - (h + 0.5t) \frac{\pi}{ka} y_6; \\ \frac{dy_3}{d\xi} &= y_4; \quad y_5 = w; \\ \frac{dy_5}{d\xi} &= y_6; \\ \frac{dy_6}{d\xi} &= y_7; \\ \frac{dy_7}{d\xi} &= y_8; \\ \frac{dy_8}{d\xi} &= -\frac{\varphi}{r} y_7 - \frac{a}{\pi r(h + 0.5t)} y_4. \end{aligned} \quad (24)$$

This system was solved numerically with the help of "Mathcad" mathematical program. For a numerical example, let  $h = 0,01$ ;  $t = 0,2$ ;  $G_3 = 3,10^5$ ;  $\mu = 0,3$ ;  $E = 2,10^{10}$

The obtained results are presented in the form of graphs in figures 6÷9, respectively.

It can be seen from this that the increase in the uniformity coefficient  $k$  leads to a decrease in the longitudinal displacement. A similar result holds for transverse displacement (Figure 8).

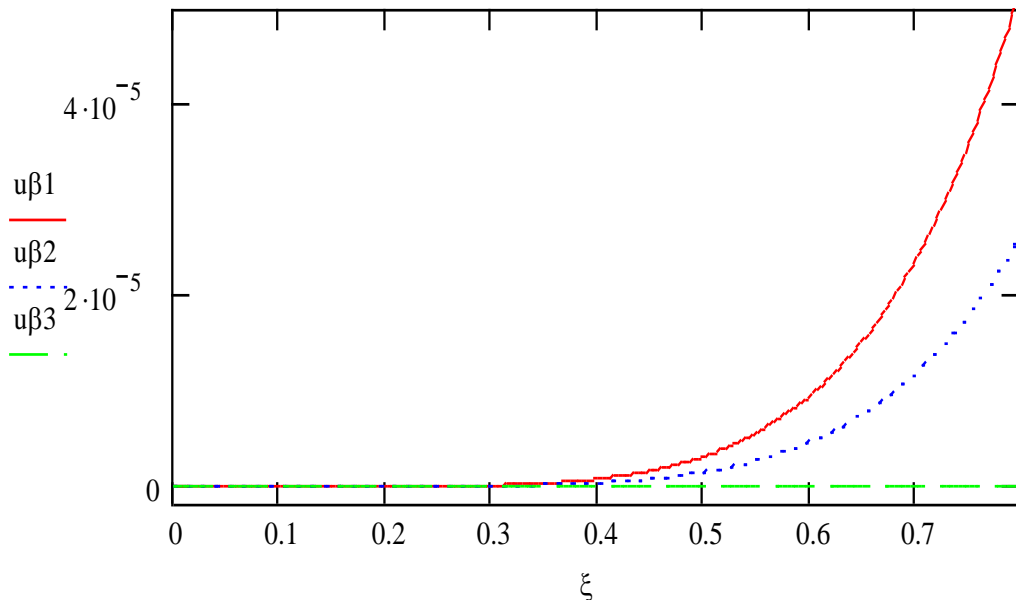
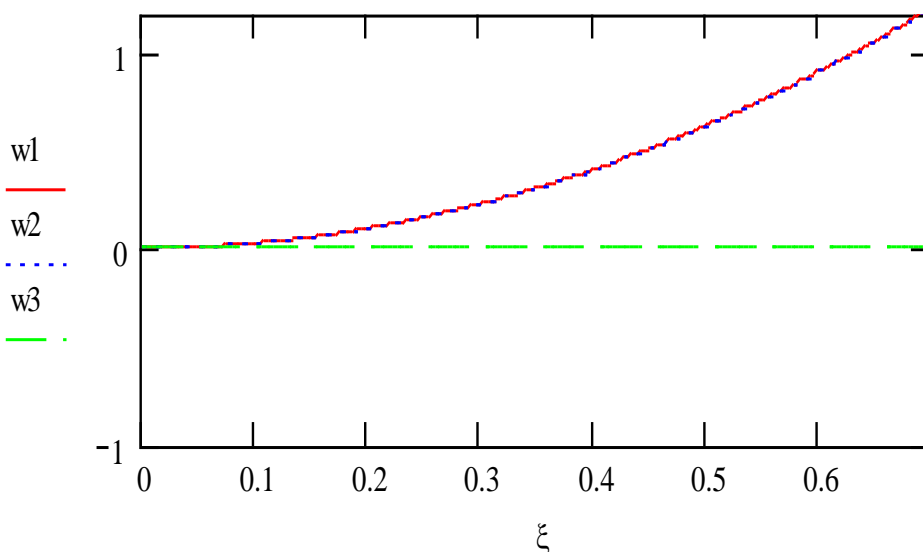


**Figure 7. Variation of displacement  $u_\beta$  as a function of  $\xi$  at different values of  $k$**



**8 pictures. Graphs representing the variation of displacement  $w$  as a function of  $\xi$  at different values of  $k$**

As mentioned above, the system (23) is solved using the Mathcad program. The calculation results are presented in the form of graphs (Fig. 8). To solve the problem, the following values of the parameters included in the system (23) were adopted:  $h = 0,01$ ;  $t = 0,02$ ;  $G_3 = 3,10^5$ ;  $\mu = 0,3$ ;  $E = 2,10^{10}$ . . Figure 9 shows the graphs representing the dependence of the critical force on the coefficient k.

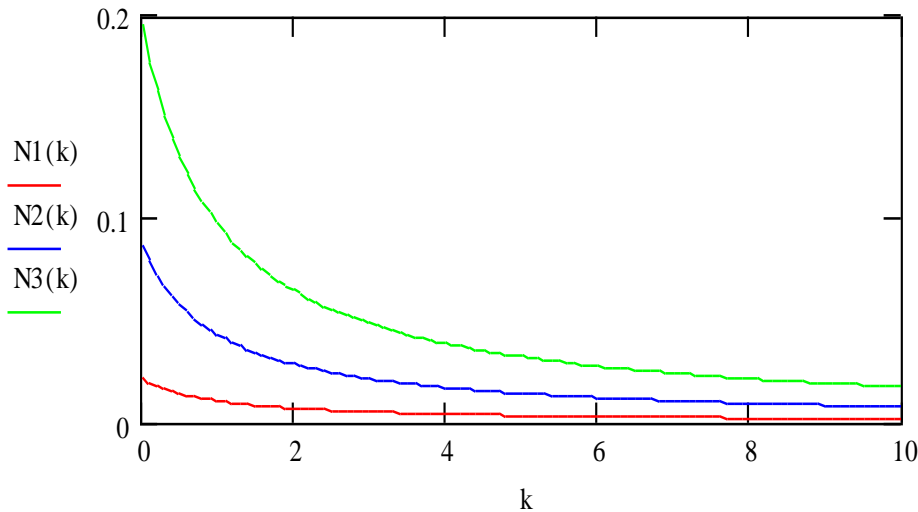


**Figure 9. Dependence of the critical force on the coefficient k (1-h=0.01; 2-h=0.03; 3-h=0.05),**

Figure 10 shows the graphs representing the dependence of displacements on the  $\xi$  coordinate.

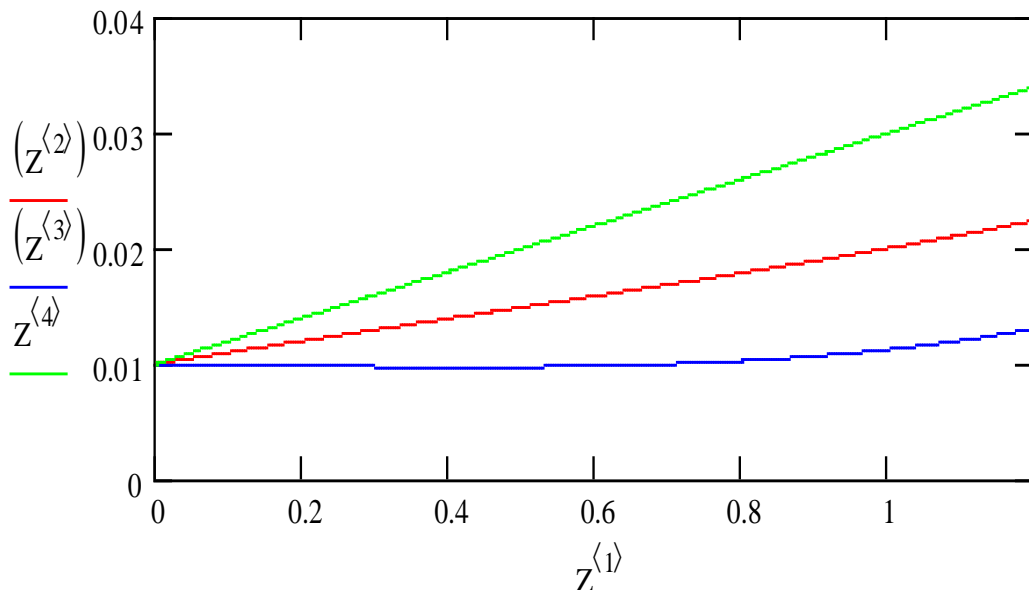


**Figure 10. Dependence of displacements**

(1-  $z^{(2)} = u_\beta$ ; 2-  $z^{(3)} = v_\beta$ ; 3-  $z^{(4)} = w$ ) ( $\xi = z^{(1)}$ )

As can be seen from the graphs, displacements have an increasing character until the critical force is reached. After that, we calculate the displacements in the layers. The calculation results are shown in Figures 11-13

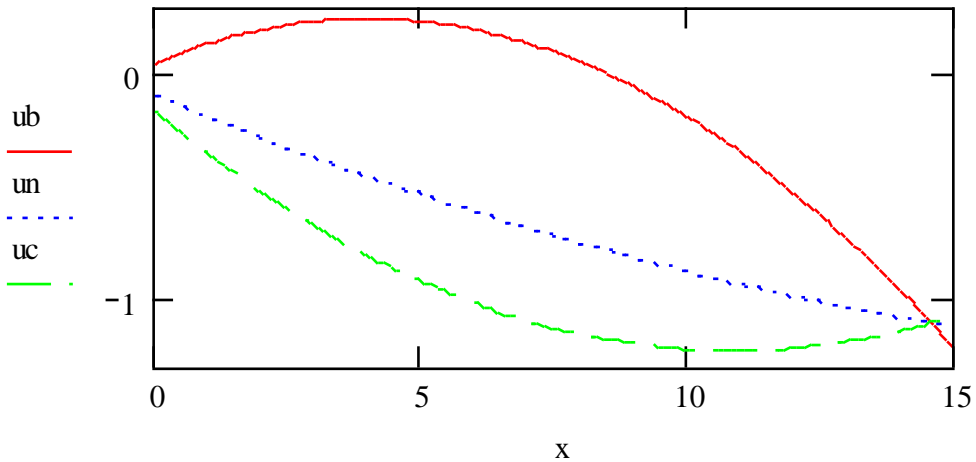


Figure 11. Graphs defining longitudinal displacements in layers, respectively, by the x coordinate

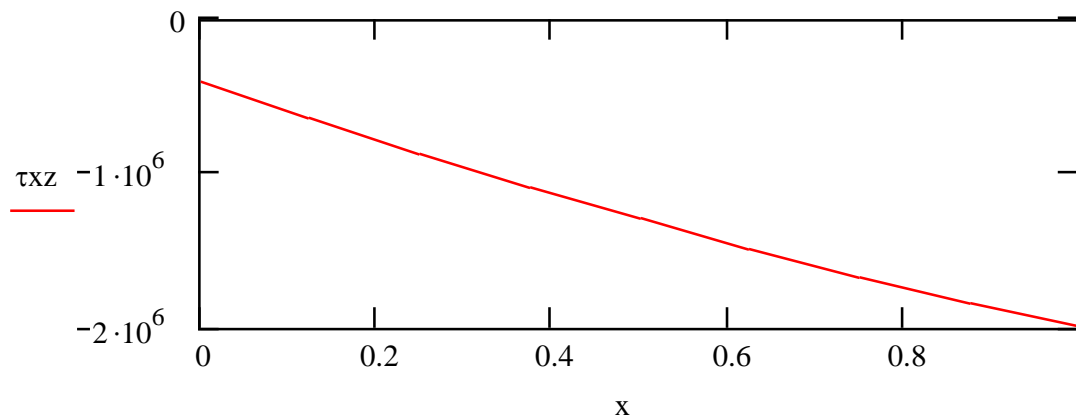
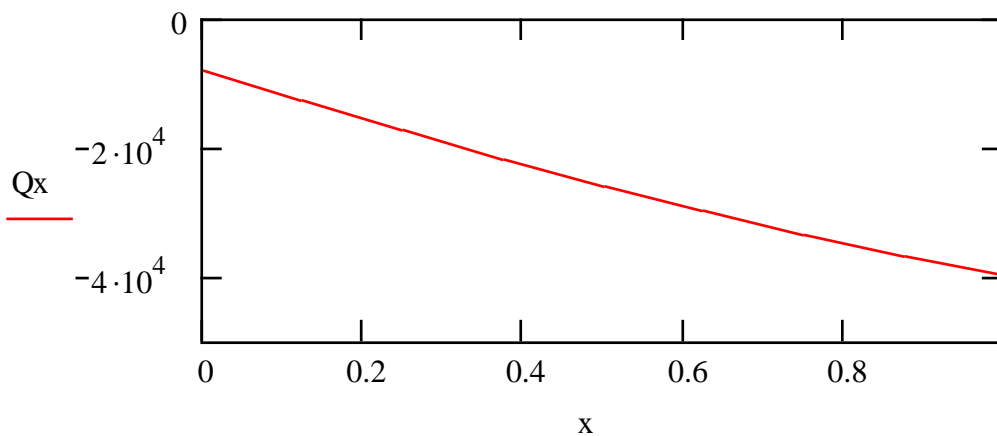


Figure 12. Graphs representing the variation of the concerning voltage in the outer layer along the x-coordinate



### Figure 13. Graphs representing the variation of the cutting force in the outer layer along the x-coordinate

Transformations in the upper layer are found in formulas

$$w_B = w_1, u_B = u_1 - (z + h + t/2) \frac{\partial w_1}{\partial x}, v_B = v_1 - (z + h + t/2) \frac{\partial w_1}{\partial y},$$

The displacements included in these formulas refer to the displacements of the upper layer  $u_1, v_1, w_1$  – and have the following form.

$$w = w_1, u_1 = u_\beta, w_2 = w_1, u_2 = -u_\beta.$$

Formulas for determining displacements for the inner layer

$$w_H = w_2, u_H = u_2 - (z - h - t/2) \frac{\partial w_2}{\partial x}, v_H = v_2 - (z - h - t/2) \frac{\partial w_2}{\partial y},$$

where  $u_2, v_2, w_2$  – characterizes the displacements in the middle layer, respectively.

The displacements in the middle layer are determined from the following formulas:

$$w_c = w, u_c = \frac{1}{2}(u_1 + u_2) - \frac{z}{2h}(u_1 - u_2 - t \frac{\partial w}{\partial x}), v_c = \frac{1}{2}(v_1 + v_2) - \frac{z}{2h}(v_1 - v_2 - t \frac{\partial w}{\partial y}).$$

Concerning voltage in the middle layer

$$\tau_{xz} = -\frac{G}{h} \left( \frac{1}{2}(u_1 - u_2) - (h + 0.5t) \frac{\partial w}{\partial x} \right)$$

is found from the formula.

Transverse force in the middle layer:

$$Q_x = -2G \left( \frac{1}{2}(u_1 - u_2) - (h + 0.5t) \frac{\partial w}{\partial x} \right)$$

Graphs of displacement, transverse force, and concerning voltage are presented in Figures 14-15

Based on the analysis of the obtained graphs, it was determined that the total displacement of the belt bushings of the thread conductor, that is, the deformation along the radius does not exceed  $(0.35 \div 0.95) \cdot 10^{-3}$  m. At the same time, it is recommended that the size of the outer belt bushing is  $(1.15 \div 1.32)$  times smaller than the size of the second layer of bushings, and the size of the third (outer) belt bushing should be  $(1.35 \div 1.45)$  times smaller than the size of the bushing.

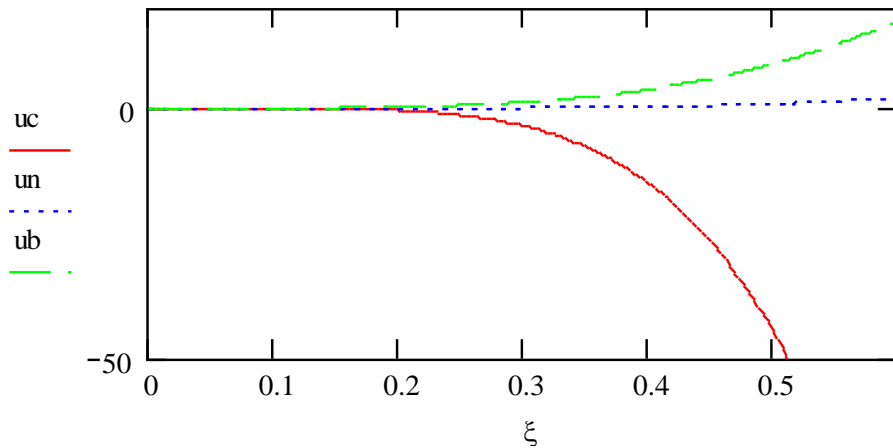


**Figure 14. Graphs representing the variation of longitudinal displacements ( $ub, un, uc$ ) in layers**

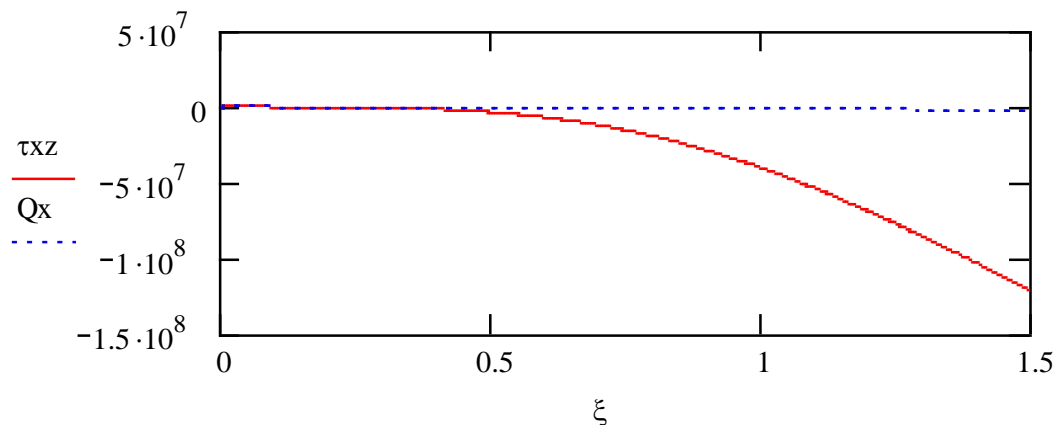


**Figure 15. Graphs characterizing the variation of the concerning voltage  $\tau_{xz}$  and the transverse force  $Q_{x\xi}$  depending on the coordinate**

*Conclusion: Mathematical expressions representing thread deformations of three-layer belt elements (bushes) of yarn transfer with different components on a ring spinning machine were obtained, connection graphs were constructed. Based on the analysis of the obtained graphs, it was determined that the total displacement of the belt bushings of the thread conductor, that is, the deformation along the radius does not exceed  $(0.35 \div 0.95) \cdot 10^{-3}m$ . At the same time, it is recommended that the size of the outer belt bushing is  $(1.15 \div 1.32)$  times smaller than the size of the second layer of bushings, and the size of the third (outer) belt bushing should be  $(1.35 \div 1.45)$  times smaller than the size of the bushing.*

### LITERATURE:

1. Razumeev K.E., Pavlov Yu.V. and others. Theoretical foundations of spinning technology // Ivanovo 2014.
2. Novichkov Yu.N., Petrovsky A.V. Stability of multilayer elastic shells // MTT, 1973, No. 1, pp. 54-56.
3. Ilyushin A.A. On averaging in systems of integro-differential equations. Dokl. AN, 1969, vol. 188, No. 1, pp. 49-52.
4. Petrovsky A.V., Laizerakh V.M. On the stability of layered shells with a viscoelastic binder // Polymer Mechanics, 1976, No. 1, 277-282 p.
5. Djumabaev G.Kh. Determination of the shape and tension of the ballooning thread, taking into account air resistance // Problems of textiles. - Tashkent, 2011, No. 3. -WITH. 53-54.
6. Djumabaev G.Kh., Abdieva G., Mavlanov T.M. Theoretical and practical basis of improvement of the yarn transfer of the ring spinning machine // TTESI Republic of Scientific-Practical Conference, Tashkent. 2012. C. 34-36.
7. Djumabaev G.Kh., Abdieva G., Mavlanov T. Mathematical modeling of the spinning process // Proceedings of the International Scientific and Practical Conference Andijan, 2012. -S.199-202.
8. Djumabaev G.Kh., Djumaniyazov K., Zhuraev A. Modeling of forced vibrations of a thread guide of a ring spinning machine // Problems of textiles. - Tashkent, 2014. No. 4. -WITH. 70-73.
9. Djumabaev G., Jumaniyazov Q., Juraev A., Gafurov Q., Mavlanov T., Gafurov J. Thread conveyor of ring spinning machine // Patent UZ No. FAP 00878. Official bulletin. -2014. - No. 2.
10. Djumaniyazov K.Zh., Juraev A., Djumabaev G.Kh., Efficient exhaust device of a spinning machine // Actual problems of innovative technologies in the conditions of integration of science education and production. Republic of Scientific-Practical Conference November 20-21, 2014. 49-52 b.
11. Djumabaev G.Kh. Influence of the improved drawing tool of the spinning machine on the geometrical properties of the yarn // Textile problems. Tashkent, 2018. No. 3. 104-108-b.
12. Djumabaev G., Djumaniyazov K., Juraev A. Spinning machine threading equipment // Patent No. FAP 01051. Official Bulletin 2015. No. 12.
13. Jumaniyazov K., Djuraev A., Djumabaev G. Substantiation of parameters' division drum with an elastic element spinning the device // European science review Vienna 2016. 11-12 November. 181-183 pages.

14. Djumabaev G., Jumaniyazov K., Matismailov S.L. Research of influence of thread guiders with flexible elements for the process of yarn formation // European science review Vienna 2018. November.

15. K. Djumaniyazov, G. Djumabaev, N. Juraeva, A. Xurramov. Analysis of Vibrations of the Rings of the Internal Spinning Machine // Cite as: AIP Conference Proceedings 2402, 070046 (2021); <https://doi.org/10.1063/5.0072022> Published Online: 15 November 2021.

16. Djumabaev G.Kh. et al. Study of the influence of an improved drawing device of a ring spinning machine on the quality of the produced yarn // Journal "Problems of textiles" Tashkent. No. 3., 2018

17. Djumabaev G.Kh., Abdieva G., Mavlanov T.M. Simulation of twist dependence of specific frequencies of untwisted textile yarns with structural exchange // Proceedings of the International Scientific and Practical Conference. - Namangan, 2012. C 199-202.